Terr. Atmos. Ocean. Sci., Vol. 19, No. 4, 331-339, August 2008 doi: 10.3319/TAO.2008.19.4.331(IMAGES)

A Late Quaternary Planktonic Foraminiferal Oxygen Isotope Record of the Banda Sea: Chronostratigraphy, Orbital Forcing, and Paleoceanographic Implications

Chih-Wei Chen[1], Kuo-Yen Wei[1,*], Horng-Sheng Mii[2], and Tien-Nan Yang[3]

[1]*Department of Geosciences, National Taiwan University, Taipei, Taiwan, ROC*
[2]*Department of Earth Sciences, National Taiwan Normal University, Taipei, Taiwan, ROC*
[3]*Institute of Earth Sciences, Academia Sinica, Taipei, Taiwan, ROC*

Received 6 September 2006, accepted 21 September 2007

ABSTRACT

A detailed oxygen isotope time-scale based on planktonic foraminifera *Globigerinoides sacculifer* at site MD012380 in the Banda Sea was established for the past 820 kyrs by correlating the record to the astronomically tuned benthic oxygen isotope chronology of MD972143. Ages for marine isotope stratigraphic (MIS) events from 2.0 back to 21.1 were designated for this western tropical Pacific record.

Spectral analysis of the $\delta^{18}O$ time-series reveals distinct periodicities of 100, 41, and 23 kyrs, indicating strong orbital forcing, yet the power of each band varies through time. The time-series of three other paleo-proxies, namely, coarse fraction (CF), lightness of sediments and $\delta^{13}C$ of *Globigerinoides sacculifer*, were subjected to cross-spectral analyses against the oxygen isotope record. The Mid-Brunhes (MIS 13 - 10, 535 - 333 ka) divides the record into two time domains characterized by different spectral behaviors. Before the Mid-Brunhes, the analyzed proxies show relatively stronger powers at the 41-kyr band, and the coherence among various proxies is relatively high. After the Mid-Brunhes, 100-kyr periodicity becomes to dominate the $\delta^{18}O$ and coarse fraction records while coherence among the various proxies becomes weaker.

The spectral behaviors of the various paleo-proxies appear to vary through the late Quaternary and are fundamentally changed by the Mid-Brunhes event, suggesting the existence of an ever changing, internally complicated system of the Banda Sea under the influence of orbital forcing during the last 820 kyrs.

Key words: Age model, Oxygen isotope stratigraphy, Quaternary, Banda Sea

Citation: Chen, C. W., K. Y. Wei, H. S. Mii, and T. N. Yang, 2008: A late quaternary planktonic foraminiferal oxygen isotope record of the Banda Sea: Chronostratigraphy, orbital forcing, and paleoceanographic implications. Terr. Atmos. Ocean. Sci., 19, 331-339, doi: 10.3319/TAO.2008.19.4.331(IMAGES)

1. INTRODUCTION

Fueled by constantly high sea-surface temperature (SST) of > 28°C (Yan et al. 1992), the Western Pacific Warm Pool (WPWP) is a key supplier of heat and moisture to the middle and high latitudes. Such a warm water pool appears to have existed in the tropical western Pacific for at least the past 1.75 million years although the SST might have lowered by as much as ~4°C during the glacial intervals (de Garidel-Thoron et al. 2005). Changes in north-south thermocline gradients of surface waters in the South China Sea as indicated by planktonic foraminiferal assemblages suggest that the WPWP was formed at about 4.0 - 3.2 Ma (Jian et al. 2006). Mounting evidence accumulated in the past decade has ranked the WPWP a leading role in modulating global climatic changes at both millennial and orbital timescales (Cane 1998). The Banda Sea, one of the Indonesian marginal seas, situated in the center of the WPWP, plays a key role in inter-ocean exchange of thermocline waters between the Pacific and Indian Ocean (Gordon 1986). However, little is known for its role in the Quaternary climate change except for a short record derived from Core SHI 9014 (7.6 m in length) for the past 180 kyrs (Ahmad et al. 1995). To fill in this void, herein we present a high-resolution multiproxy record form a long piston core, MD012380 (126°54.25E, 05°45.64S, Fig. 1), retrieved from the Banda Sea during 2001.

* *Corresponding author*
E-mail: weiky@ntu.edu.tw

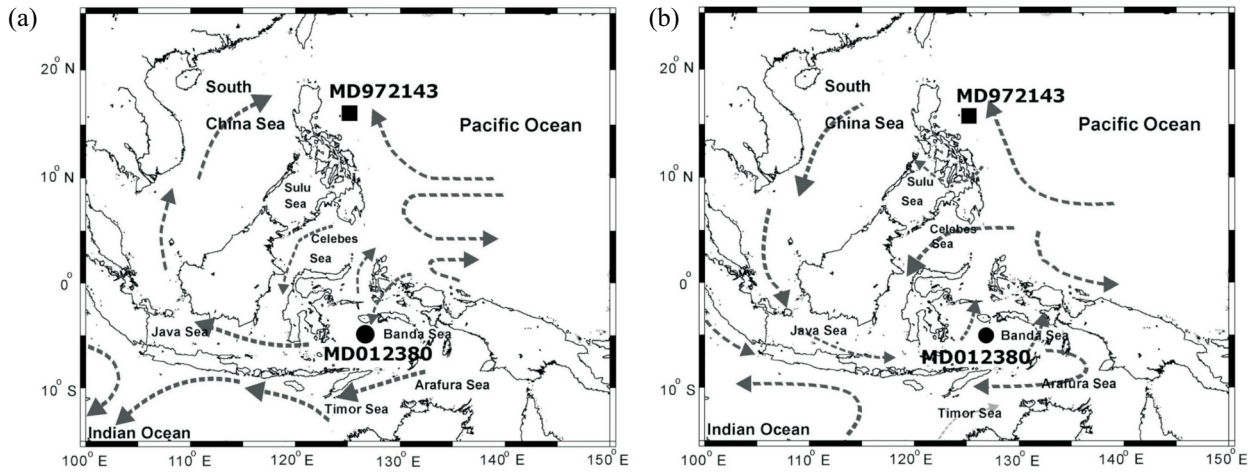

Fig. 1. Map showing the locations of sites mentioned in the text and surface water circulation patterns in the Indonesian Seas (modified after Wyrtki 1961; Ahmad et al. 1995). (a) Dotted arrows indicate the surface-water flow pattern during the southeast monsoon season (from May to September). (b) Dotted arrows indicate the surface-water flows during the northwest monsoon season (from November to March).

At present, the surface water circulations in the Banda Sea and adjoining areas are mainly driven by the seasonally reversing monsoonal winds (Fig. 1). From November to March during the austral summer, the northwest monsoon prevails, the surface water flows from the Java Sea into the Banda Sea. During the winter, the southeast monsoon drives the surface current in an opposite direction from the Banda Sea and Arafura Sea to the Java Sea. Meanwhile, the Pacific deep water is transported as thermocline water to the Indian Ocean via the Indonesian seas. The magnitude of the thermocline water export during the southeast monsoon is enhanced by a factor of 3 to 4 times (Wyrtki 1957, 1961, 1987; Murray and Arief 1988).

During the glacial intervals when the sea level dropped, the geographic configuration of land and sea distribution was significantly different from today's. The sea-level drop not only reduced the extent of the surface ocean (Wang 1999) but also closed certain passages between islands and therefore changed the ocean circulation patterns in the various marginal seas as well as the flow routes and flux of the Indonesian Throughflow. Ahmad et al. (1995) suggested that the surface and bottom waters in the Banda Sea had higher salinity during the glacial intervals while the change has been influenced by the precession (23-kyr periodicity). Furthermore, the carbonate content in bulk sediments increased during the glacial periods as a result of deepening of the lysocline of the Pacific Ocean in general.

Core MD012380 was taken from the Banda Sea at a water depth of 3232 m during 2001 MD122/IMAGES VII Cruise of the IMAGES (**I**nternational **Ma**rine **G**lobal Change **S**tudy) Project (Bassinot and Baltzer 2001). Here we present planktonic oxygen and carbon isotopic variations, coarse-fraction percentage and color reflectance of bulk sediments in an attempt to: (1) establish an astronomically tuned chronology for the record; and then (2) characterize the periodicity of the records and their cross-relationships.

2. METHODS

2.1 Oxygen and Carbon Isotopic Analyses

For stable oxygen and carbon isotopic analyses, samples were taken every 10 cm as to reach a temporal resolution of at least 1 sample per 2.5 kyrs. A total of 20 - 30 well-preserved specimens of planktonic foraminifera *Globigerinoides sacculifer* in the size fraction of 355 - 425 μm were picked from each sample. Besides visual inspection under light microscopes, the preservation state of selected specimens was double checked by SEM to make sure that the specimens were not affected by dissolution or overgrowth of calcite.

The picked specimens were first cleaned with ultrasonic vibration in ethanol solution and sodium hypochlorite solution. A total of 5 - 6 foraminiferal foraminifers were then reacted with phosphoric acid at 90°C in an automation system of Micromass Multicarb. The CO_2 gas yielded was analyzed with Micromass IsoPrime isotope spectrometer in the Department of Earth Sciences, National Taiwan Normal University. The NBS-19 was used as a calibration standard ($\delta^{13}C$ = +1.95‰, $\delta^{18}O$ = -2.20‰). The external precision of the measurement of NBS-19 was 0.04‰ for $\delta^{13}C$ and 0.06‰ for $\delta^{18}O$, respectively.

2.2 Color Reflectance and Coarse Fraction

The color reflectance of sediments was measured with spectrophotometer Minolta 2022 on shipboard at 2-cm intervals. In this study, we chose lightness (equivalent to grayscale reflectance) for its effectiveness to display high frequency variation (Chapman and Shackleton

1998). A 1-cm increment was chosen for down core signal sampling. The content of coarse fraction (> 63 μm) of sediment were weighted using sieved sediments at 5-cm intervals. The coarse fraction is dominantly made of foraminiferal tests.

2.3 AMS-C^{14} Dating

To establish a reliable chronology for the past 20 kyrs, foraminifers from five specific depths in the upper 5 m of the core were used for AMS-^{14}C dating. In each sample, more than 200 individuals of *G. sacculifer* and *G. ruber* in the size range of 355 - 425 μm were picked, cleaned and sent to the Rafter Radiocarbon Laboratory, Institute of Geological and Nuclear Sciences, New Zealand for AMS dating.

2.4 Power Spectrum Analysis

To find the periodicities as well as the coherence and phase relationships among the measured proxies, we used the Analyseries 2.0.3 software (available at: http://www.lsce.cnrs-gif.fr/soft-lsce/index-en.html) to perform various time-series analyses.

3. RESULTS AND DISCUSSIONS

3.1 The Age Model of MD012380

The age model of MD012380 is established based upon four kinds of control points (Table 1). Five AMS-C^{14} dating points calibrated by CALIB 4.3 software (by Stuiver and Reimer, executed at http://calib.qub.ac.uk/calib/) into calendar ages were used for tying the last 20 ka. Fitting with the benthic foraminiferal oxygen isotope stratigraphy of MD 972143 in the Western Philippine Sea (Horng at al. 2002), marine isotope stages 1 - 21 were unequivocally identified in MD012380 by amplitude variation in the $\delta^{18}O_{sacculifer}$ profile. Besides its proximity to our studied site, MD972143 is also advantageous in having a well-defined, high resolution, open-ocean, astronomically tuned benthic foraminiferal $\delta^{18}O$ record augmented with excellent magnetostratigraphic and biostratigraphic controls (Horng et al. 2002). The last occurrence of *Pseudoemiliania lacunosa* in MD012380 was observed at 2840 cm and designated as 458 ka in age (Thierstein et al. 1977). The Brunhes/Matuyama boundary

Table 1. Depth-age pairs in MD012380 based upon four kinds of age controls, including AMS-^{14}C dating, $\delta^{18}O$ graphic fitting, the Last Occurrence of *Pseudoemiliania lacunosa* (LO P.l.), and the Brunhes/Matuyama boundary (Huang 2003). Corresponding plots of age-depth relationship and sedimentation rates are shown in Fig. 3.

Depth (cm)	Age (ka)	Method	Depth (cm)	Age (ka)	Method	Depth (cm)	Age (ka)	Method
41	4.2	AMS-^{14}C Dating	2071	254.8	Correlated to the benthic $\delta^{18}O$ record of MD972143	3221	575.0	Correlated to the benthic $\delta^{18}O$ record of MD972143
111	7.7		2101	268.0		3261	586.4	
191	14.6		2211	287.8		3371	600.1	
301	18.3		2381	315.3		3421	617.3	
411	23.6		2461	336.7		3461	631.0	
581	37.7	Correlated to the benthic $\delta^{18}O$ record of MD972143	2581	364.5		3501	648.1	
691	50.9		2611	378.0		3541	665.2	
871	67.6		2691	400.5		3631	689.2	
971	81.5		2731	411.8		3651	699.5	
1251	109.3		2761	416.3		3701	724.2	
1451	130.1		2811	434.7		3731	736.9	
1571	146.1		2881	469.3		3771	749.6	
1691	169.8		2911	474.9		3781	758.0	
1711	184.0		2951	492.3		3821	773.6	
1781	197.0		2971	501.0		3881	783.0	
1851	217.5		3011	510.0		3911	787.8	
1901	221.6		3021	525.0		3931	792.7	
1931	225.7		3091	538.2		3971	821.7	
1991	240.0		3131	545.0		2840	458.0	LOP.l.
2061	246.6		3181	558.6		3870	781.3	B/M

in this core recognized from geomagnetic analysis (Huang 2003, unpublished master thesis) provides another independent control point for chronology. In addition, the last appearance depth of pink *G. ruber* at 1461 cm marks an age of ~131 ka (Lee et al. 1999; Wei et al. 2003). More details will be discussed in section 3.3.

3.2 Sedimentation Rates

The sedimentation rates of MD012380 vary from 1 to 29 cm kyr^{-1} during the past 820 kyr (Fig. 3b). An abrupt increase from 5 to 20 cm kyr^{-1} in the upper part of the core is attributed to an over-sampling of sediments caused by the piston coring process of the Calypso core (Széréméta et al. 2004). Overall, sedimentation rates decrease downcore by the effect of weight compaction. The calculated average sedimentation rate of 4.8 cm kyr^{-1} is consistent with the previous result in this area (Ahmad et al. 1995). The sedimentation rates do not vary with glacial-interglacial alternations, suggesting that the sea-level changes induced by ice-volume do not significantly affect sedimentation during the studied period.

3.3 Planktonic Foraminiferal Oxygen Isotope Stratigraphy

A long planktonic foraminiferal $\delta^{18}O$ record in the Banda Sea was established at 5-cm intervals for the upper 450 cm and at 10-cm resolution for the lower sections (Fig. 2). The $\delta^{18}O$ values vary between -0.5 ~ -2.5‰, attributable to SST change, ice-volume effect and local salinity variation. MIS 1 - 21 were clearly identified (Fig. 4). However, some sub-stage $\delta^{18}O$ features in this high resolution record of MD012380 are not readily correlated with features in the SPECMAP profile, nor the low-latitude stack of Bassinot et al. (1994). Here we choose a benthic oxygen isotope record from MD972143 as the target for curve matching. The benthic $\delta^{18}O$ record of MD972143 was generated from *Cibicidoides wuellerstorfi* (Lee et al. 2001) and correlated to an astronomically tuned composite record of Cores V19-30, ODP677, and 846 (named as V677846, available at http://delphi.esc.cam.ac.uk/coredata/v677846.html) (Horng et al. 2002). Because the benthic environment is more stable in hydrology than the surface waters, the benthic record supposedly reflects mainly the global ice-volume change through time. The resultant timescale was then re-tuned against the astronomical resolution of La93 (1.1) (Laskar et al. 1993) and resulted in a 2.15 Ma timescale augmented with excellent magnetostratigraphy and biostratigraphic controls (Horng et al. 2002).

We followed the taxonomy established in SPECMAP stack (Imbrie et al. 1984) to designate oxygen isotopic stages and sub-stages. The high resolution of our record at MD 012380 allows us to identify a few new sub-stages that were not clearly marked in the previous stacks. We denominated these sub-substages by the principle of assigning even numbers for colder intervals and odd numbers for warmer ones. With these newly added sub-stages, a revised western Pacific marine oxygen isotope chronology for the past 0.82 Myr was proposed (Fig. 4) and all the recognized oxygen isotopic events are listed in Table 2.

At about 400 ka, at the transition from MIS 12 to MIS 11, the $\delta^{18}O$ shows the largest rise in amplitude during the past 6 Myr (Droxler and Farrell 2000). This also marks the peak time of the so-called Mid-Brunhes Events (MBE). The MBE is characteristic by showing asymmetric climate patterns

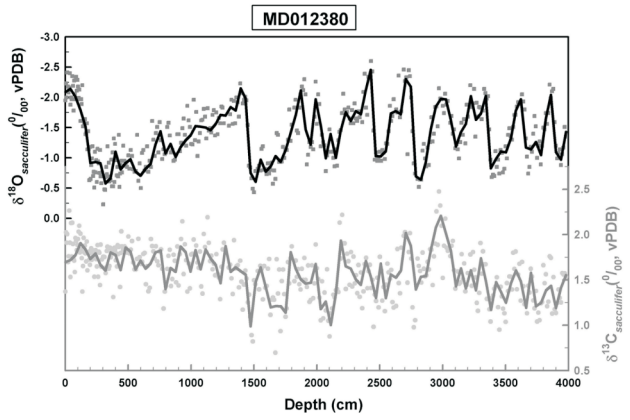

Fig. 2. Raw data of $\delta^{18}O$ (square dots) and $\delta^{13}C$ (circle dots) in MD012380 plotted against core depth. Smoothed trends are represented by thick curves respectively. Note that the scale of $\delta^{18}O$ on the left axis is different from the scale of $\delta^{13}C$ on the right axis.

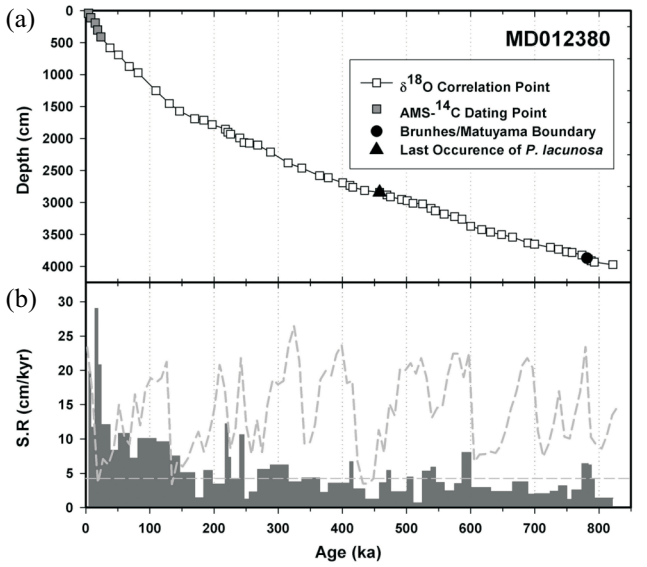

Fig. 3. (a) Age-depth relationship of core MD012380. Filled squares represent AMS-^{14}C dating points. Hollow squares are $\delta^{18}O$ fitting points correlated to MD972143. The filled circle indicates the geomagnetic B/M boundary (Huang 2003). The triangle represents the LO of *P. lacunosa*. (b) Sedimentation rates of MD012380 for the last 800 ka. Horizontal dashed line indicates the mean sedimentation rate of 4.82 cm kyr^{-1}. Dashed curve represents the smoothed $\delta^{18}O$.

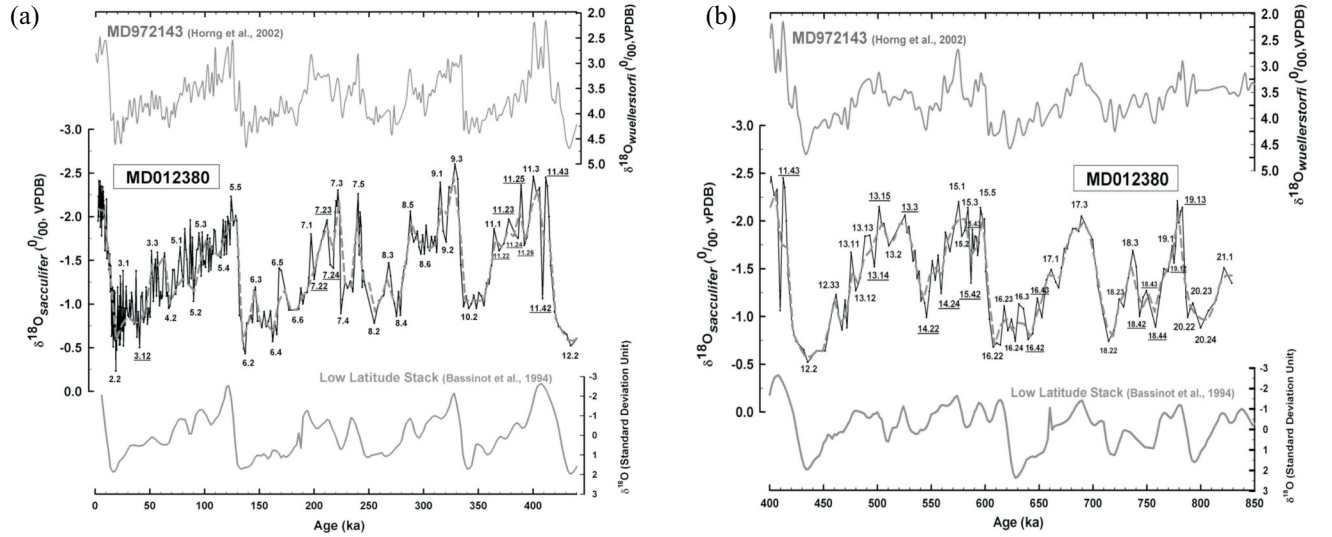

Fig. 4. (a) MIS 1 - 11 $\delta^{18}O$ stratigraphy of MD012380 correlated with that of MD972143. The dash curve represents the smoothed trend. Numbers indicate the marine isotope stages recognized in MD012380. Revisions of substages differing from the SPECMAP stack are marked with underlines. Low Latitude Stack (Bassinot et al. 1994) in the bottom panel was chosen for comparison for its comparable age and latitudinal closeness. Detailed ages of MIS events in MD012380 are listed in Table 2. (b) MIS 20 - 11 $\delta^{18}O$ stratigraphy of MD012380 correlated with that of MD972143. The dash curve represents the smoothed trend. Numbers indicate the marine isotope stages recognized in MD012380. Revisions of substages differing from the SPECMAP are marked with underlines. Low Latitude Stack (Bassinot et al. 1994) in the bottom panel was chosen for comparison for its comparable age and latitudinal closeness. Detailed ages of MIS events in MD012380 are listed in Table 2.

Table 2. Marine isotope events in MD012380 based on correlation to the astronomically-tuned chronology of oxygen stratigraphy of MD972143 (Horng et al. 2002). Newly designated substages which were not recognized in the SPECMAP stack are marked with italic font.

event	age (ka)	event	age (ka)	event	age (ka)	event	age (ka)
2.0	12.0	7.3	221.6	*11.43*	*411.8*	16.23	617.3
2.2	18.3	7.4	224.3	12.0	417.7	16.24	627.5
3.0	21.6	7.5	240.0	12.2	434.7	16.3	631.0
3.1	24.9	8.0	247.4	12.33	461.0	*16.42*	*639.5*
3.12	*40.1*	8.2	254.8	13.0	473.0	*16.41*	*648.1*
3.3	50.9	8.3	268.0	13.11	474.9	17.0	656.7
4.0	57.4	8.4	275.2	13.12	479.3	17.1	660.9
4.2	66.7	8.5	287.8	13.13	492.3	17.3	689.2
5.0	74.1	8.6	300.7	*13.14*	*496.7*	18.0	701.8
5.1	77.3	9.0	313.6	*13.15*	*501.0*	18.22	714.3
5.2	89.4	9.1	315.3	13.2	510.0	18.23	724.2
5.3	97.4	9.2	320.6	*13.3*	*525.0*	18.3	736.9
5.4	114.5	9.3	328.6	14.0	535.0	*18.42*	*743.2*
5.5	123.9	10.0	332.6	*14.22*	*545.0*	*18.43*	*749.6*
6.0	131.8	10.2	336.7	*14.24*	*558.6*	*18.44*	*758.0*
6.2	136.8	11.0	359.9	15.0	566.8	19.0	765.8
6.3	146.1	11.1	364.5	15.1	575.0	19.1	773.6
6.4	161.9	*11.22*	*369.0*	15.2	577.9	*19.12*	*775.2*
6.5	167.8	*11.23*	*378.0*	15.3	583.6	*19.13*	*783.0*
6.6	184.0	*11.24*	*386.4*	*15.42*	*586.4*	20.0	785.4
7.0	190.5	*11.25*	*389.3*	*15.43*	*587.7*	20.22	787.8
7.1	197.0	*11.26*	*392.1*	15.5	595.2	20.23	792.7
7.22	*199.9*	11.3	400.5	16.0	601.1	20.24	799.9
7.23	*211.6*	*11.42*	*408.9*	16.22	607.0	21.1	821.7
7.24	*217.5*						

between Northern and Southern hemispheres (Jansen et al. 1986; Pisias and Rea 1988), such that the northern hemispheric climate became more or less 'glacial' whereas the southern hemisphere turned more toward interglacial conditions. Here in the southern equatorial Pacific, the termination of glacial stage MIS 12 is marked by a ~2.0‰ rise in $\delta^{18}O$, which is, however, similar in amplitude to the concomitant rise seen in the benthic $\delta^{18}O$ record (Fig. 5a). Such a co-varying change in both planktonic and benthic δ^{18} values seems to suggest that the MIS 12 - 11 transition is caused by a major ice melting.

3.4 $\delta^{13}C$ Maximum and Preservation of Carbonates

The $\delta^{13}C$ profile is characterized by a moderate glacial-interglacial fluctuation pattern. Generally speaking, the interglacial intervals tend to have high values and vice versa. The overall pattern is consistent with most previous planktonic and benthic foraminiferal $\delta^{13}C$ profiles (Wang et al. 2004) in showing an ever rising trend from 800 ka, culminating to a maximum at ~500 ka, and then a declining trend until the end of MIS 6 at about 130 ka. The maximum at ~500 ka has been considered a precursor to the MBE (Wang et al. 2004).

Coarse fraction (> 63 μm) in MD012380, which mostly consists of biogenous carbonate grains such as foraminifera tests, shows generally a good correlation with lightness of the bulk sediments (Figs. 5d, e). Variation of coarse fraction (CF) is considered a good indicator of carbonate preservation. The relatively higher CF values during the glacial inter-

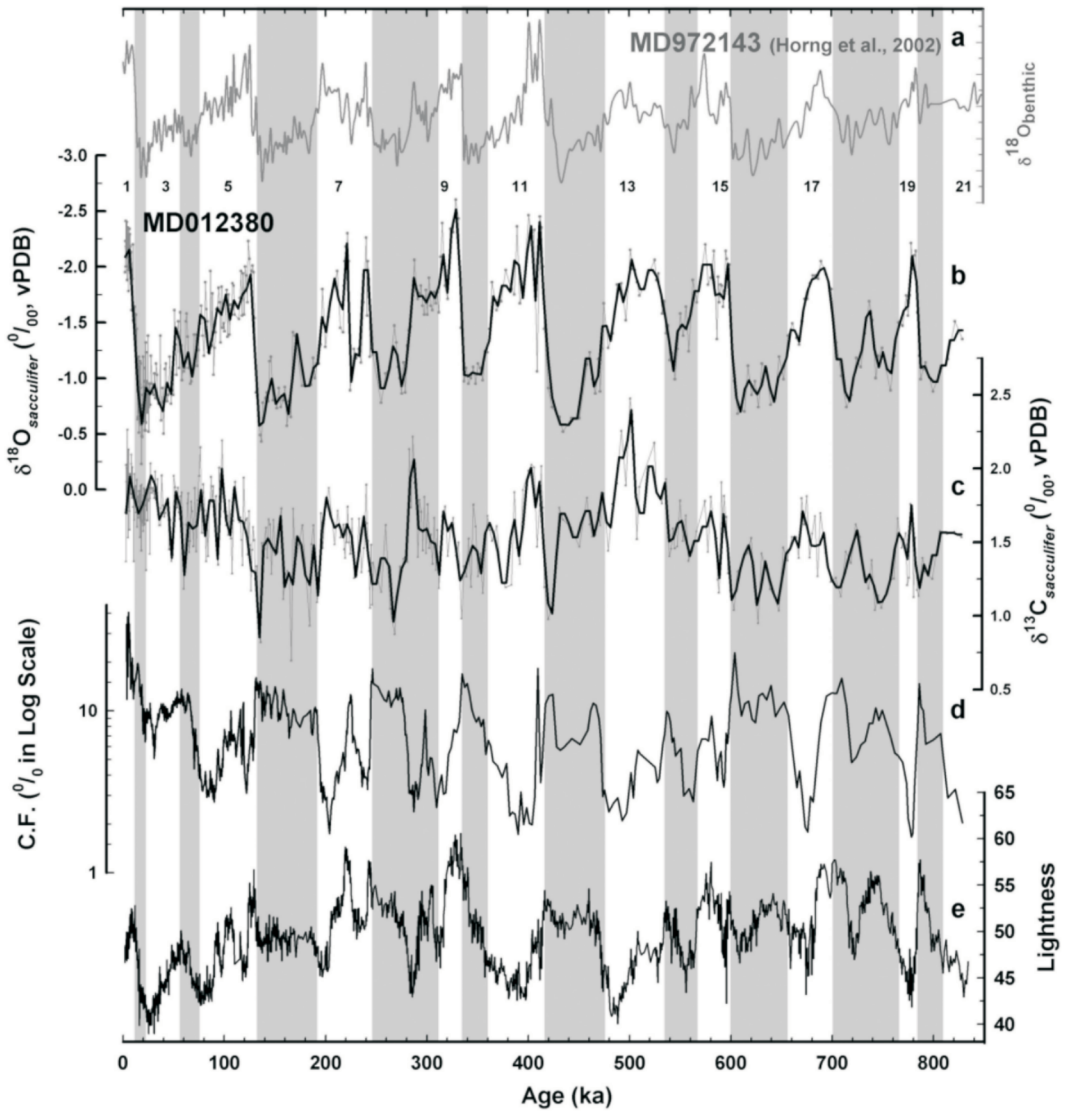

Fig. 5. Plots of various proxies against age. Gray bars mark the glacial intervals. (a) $\delta^{18}O$ of MD972143 from benthic foraminifera *Cibicidoides wuellerstorfi* (Horng et al. 2002) as the target curve for correlation. (b) - (e) are paleo-proxies in MD012380 shown as: (b) $\delta^{18}O$ vs. age for core MD012380, thick line represents the running average; (c) $\delta^{13}C$ vs. age, thick line represents the running average; (d) percentage of coarse fraction (C.F. %, in log scale) vs. age; (e) lightness of sediment vs. age. Note that the Y-axes are at different scales in each plot. Numbers on panel (b) indicate the MIS events.

vals result from better preservation of foraminiferal tests, attributed to less corrosive bottom waters when the lysocline deepened in the equatorial Pacific (Farrel and Prell 1988; Ahmad et al. 1995). The better preservation of carbonate during the glacial intervals also causes the sediments brighter in color and therefore results in higher lightness values (Figs. 5d, e). Nevertheless, in several intervals, the brightness peak lags slightly behind the CF peak (for example, at 690, 590, and 330 ka). This apparent discrepancy is likely caused by aliasing due to the lower resolution of the CF record (half of that of the lightness data).

3.5 Spectral Analyses of the Time-Series of $\delta^{18}O$, $\delta^{13}C$, Coarse Fraction and Lightness

The spectrogram of $\delta^{18}O$ variation reveals clearly the dominance of three major Milankovitch's cycles of 100-, 41-, and 23-ky periods (Fig. 6), attesting that the variation in planktonic $\delta^{18}O$ was modulated predominantly by ice-volume with some precession-driven changes in temperature and salinity. To investigate the relationship among the various proxies, we preformed cross-spectral analysis for each pair of proxies in the three possible combinations. Many previous studies (e.g., Droxler and Farrell 2000; Berger and Loutre 2003; Wang et al. 2004) have shown that the MIS 13 - 10 during the Mid-Brunhes Event are unique in various aspects and therefore are atypical to the rest of the late Quaternary, we separated the time-series into several segments for analyses; for instance, segments of MIS 21 - 14, MIS 13 - 10, MIS 21 - 10, and MIS 9 - 1. The results are shown separately in Fig. 7.

The coarse fraction shows an in-phase relationship with the $\delta^{18}O$ with strong coherence at the 100-ky band. High coherence at the 41-ky band only shows up during MIS 21 - 10 but with a lead-lag relationship (Fig. 7b). This means that the high coarse fraction would coincide with heavier $\delta^{18}O$ values (Fig. 5); this is consistent with many previous studies that show the preservation state of carbonate in the deep-sea Pacific is governed mainly by ice-volume related changes in sea-level, biological productivity and thermohaline circulation. Lightness of sediments, albeit its tendency reflect the carbonate content tied with CF, shows different spectral characteristics from CF. The lightness shows a strong power at 41-ky band during MIS 21 - 14 (Fig. 7d), but does not show 100-ky periodicity during MIS 9 - 1 (Fig. 7a). Instead, lightness of sediments shows a long-term declining trend during MIS 9 - 1 despite CF increasing remarkably during the same period (Fig. 5). This decoupling can only be explained by the following: although the foraminifera became better preserved, the sediments contain more clay and organic matter and therefore show darker coloring.

As mentioned in the previous section, the $\delta^{13}C$ time-series shows mainly long-term trends or cycles longer than a 100-ky period as elegantly discussed in Wang et al. (2004). Only during MIS 21 - 14 does $\delta^{13}C$ show a noticeable power concentration in 41-ky band (Fig. 7d.). On the other hand, the variation of $\delta^{13}C$ does not show any noticeable coherence with that of $\delta^{18}O$.

4. SUMMARY

By correlating the *G. sacculifer* $\delta^{18}O$ curve at MD 012380 with the astronomically tuned benthic $\delta^{18}O$ record at MD972143 of the Philippine Sea, we established a high-resolution oxygen isotope chronology for the past 830 kyrs for the Banda Sea. Several new sub-stages of oxygen isotopic events were recognized and designated. The lightness index of sediments varies in concert with coarse fraction, reflecting the preservation state of carbonate as a common factor for both proxies. The maximum of $\delta^{13}C$ values preceded the Mid-Brunhes Event, suggesting that the changes in the carbon cycle might be a precursor leading to the major climatic perturbation manifested by the MBE. Cross Spectral analyses revealed that brightness and CF tend to show high coherence with $\delta^{18}O$ at 100-ky band. On the other hand, $\delta^{13}C$ has its own spectral behavior.

Acknowledgements This study is a contribution to the Taiwan IMAGES project. We thank the scientific party of WEPAMA, MD122/IMAGES VII for coring in the Banda Sea. Curation of the IMAGES cores was conducted by the Core Laboratory under the National Center for Ocean Research (NCOR). Two anonymous reviewers' constructive comments greatly helped to improve our manuscript. This study was supported by National Science Council of the ROC under Grant NSC 91-2116-M-002-013 to KYW.

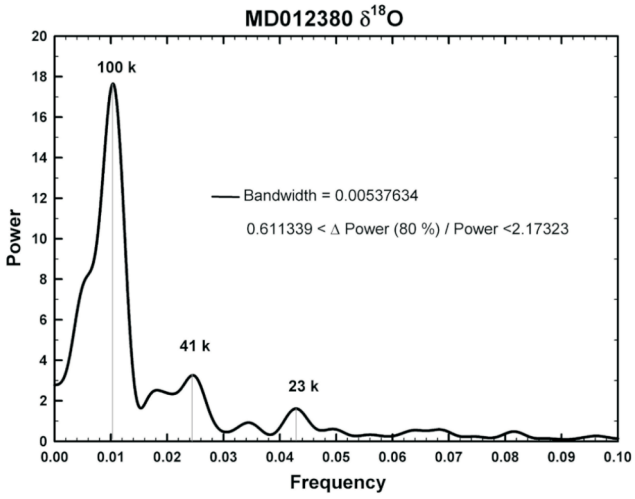

Fig. 6. Power spectrum of $\delta^{18}O$ of MD012380. Three major orbital periods of 100, 41, and 23 kyr are resolved.

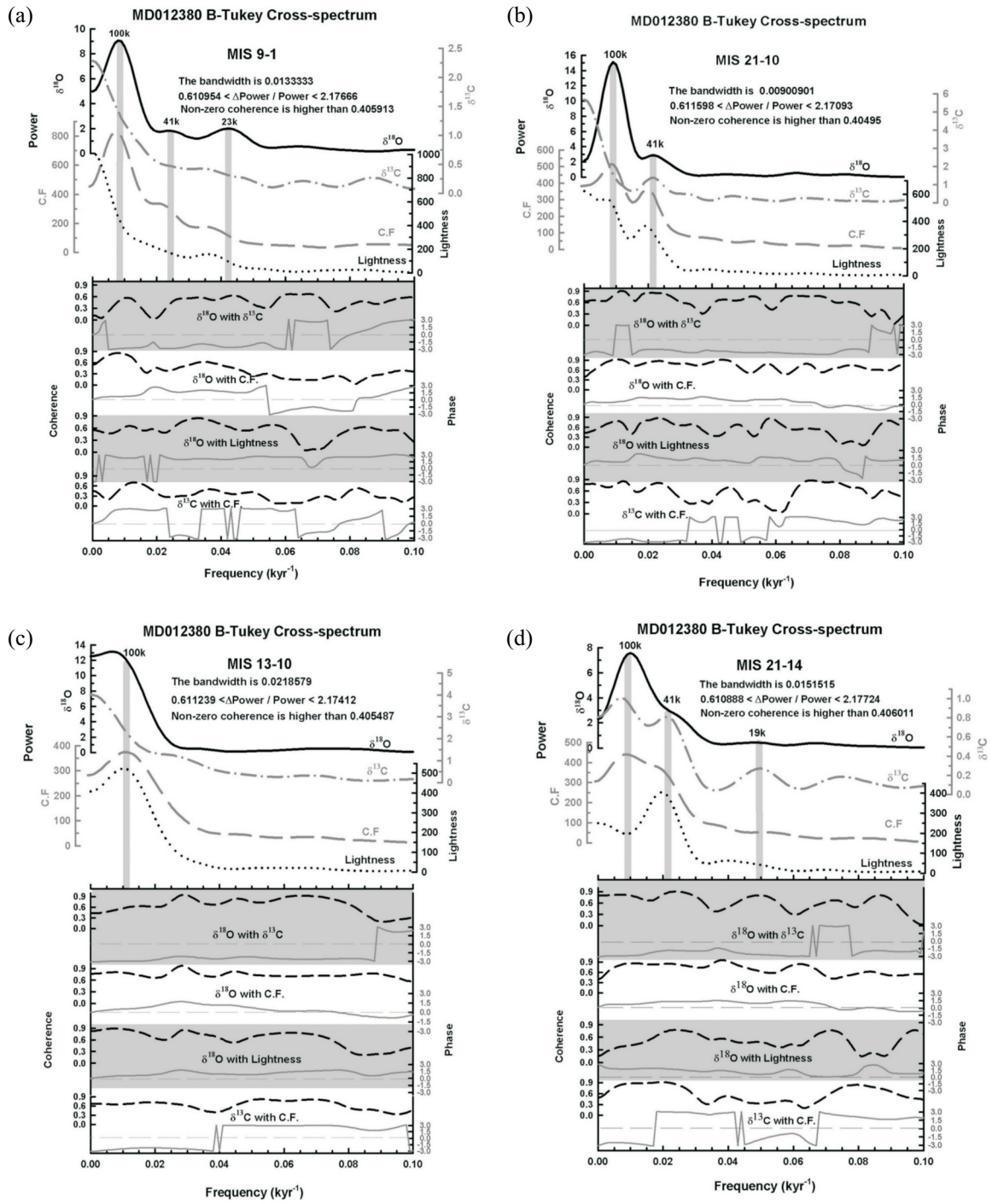

Fig. 7. Cross spectral analyses of 4 paleo-proxies in MD012380 within 4 different time durations (a) MIS 9 - 1, (b) MIS 21 - 10, (c) MIS 13 - 10, (d) MIS 21 - 14. Powers of $\delta^{18}O$, $\delta^{13}C$, C.F. and lightness are presented by four curves. Both the bandwidth and non-zero coherence are shown in each plot. Note that the power scale is different for each proxy. Notable orbital periods are marked by vertical lines.

REFERENCES

Ahmad, S. M., F. Guichard, K. Hardjawidjaksana, M. K. Adisaputra, and L. D. Labeyrie, 1995: Late Quaternary paleoceanography of the Banda Sea. *Mar. Geol.*, **122**, 385-397.

Bassinot, F., L. D. Labeyrie, E. Vincent, X. Quidelleur, N. J. Shackleton, and Y. Lancelot, 1994: The astronomical theory of climate and the age of the Brunhes-Matuyama magnetic reversal. *Earth Planet. Sci. Lett.*, **126**, 91-108.

Bassinot, F. C. and A. Baltzer., 2001: Les rapports des campagnes à la mer – WEPAMA Cruise MD122/IMAGES VII on board RV "Marion Dufresne".

Berger, A. and M. F. Loutre, 2003: Climate 400,000 years ago, a

key to the future? 17-26. In: Droxler, A. W., R. Z. Poore, and L. H. Bruckle (Eds.), Earth's Climate and Orbital Eccentricity: The Marine Isotope Stage 11 Question, *Geophy. Monogr. Ser.*, **137**, AGU, Washington DC, 240 pp.

Cane, M. A., 1998: Climate change: A role for the tropical Pacific. *Science*, **282**, (5386), 59-61.

Chapman, M. R. and N. J. Shackleton, 1998: What level of resolution attainable in a deep-see core? Results of a spectrophotometer study. *Paleoceanography*, **13**, 4, 311-315.

de Garidel-Thoron, T., Y. Rosenthal, F. Bassinot, and L. Beaufort, 2005: Stable sea surface temperatures in the western pacific warm pool over the past 1.75 million years. *Nature*, **433**, 294-298.

Droxler, A. W. and J. W. Farrell, 2000: Marine Isotope Stage 11 (MIS11): New insights for a warm future. *Global Planet. Change*, **24**, 1-5.

Farrel, J. W. and W. L. Prell, 1988: Climatic changes and $CaCO_3$ preservation: An 800,000 year bathymetric reconstruction from the central equatorial Pacific. *Paleoceanography*, **4**, 447-466.

Gordon, A., 1986: Interocean exchange of thermocline water. *J. Geophys. Res.*, **91**, 5037-5046.

Horng, C. S., M. Y. Lee, H. Palike, K. Y. Wei, W. T. Liang, Y. Iizuka, and M. Torii, 2002: Astronomically calibrated ages for geomagnetic reversals within the Matuyama chron. *Earth Planets Space*, **54**, 679-690.

Huang, Y. S. 2003: Geomagnetic study of Core MD021380 from Banda Sea: Paleoenvironmental changes of the equatorial warm pool during the past 800 thousand years. Master's thesis, National Central University, 88 pp (in Chinese).

Imbrie, J., J. D. Hays., D. G. Martinson, A. McIntyre, A. C. Mix, J. J. Morley, N. G. Pisias, W. L. Prell, and N. J. Shackleton, 1984: The orbital theory of Pleistocene climate: Support from a revised chronology of the marine $\delta^{18}O$ record. In: Berger, A., J. Imbrie, H. Hays, G. Kukla, and B. Saltzman (Eds.), Milankovitch and Climate: Understanding the Response to Astronomical Forcing, 269-305, D. Reidel, Norwell, Massachusetts.

Jansen, J. H. F., A. Kuijpers, and S. R. Troelstra, 1986: A mid-Brunhes climatic event: Long-term changes in global atmosphere and ocean circulation. *Science*, **232**, 619-622.

Jian, Z., Y. Yu, B. Li, J. Wang, X. Zhang, and Z. Zhou, 2006: Phase evolution of the south-north hydrographic gradient in the South China Sea since the middle Miocene. *Palaeogeogr. Palaeoclimatol. Palaeoecol.*, **230**, 251-263.

Laskar, J., F. Joutel, and F. Boudin, 1993: Orbital, precessional, and insolation quantities for the Earth from -20 Myr to +10 Myr. *Astron. Astrophys*., **270**, 52-533.

Lee, M. Y., K. Y. Wei, and Y. G. Chen, 1999: High resolution oxygen isotope stratigraphy for the last 150,000 years in the southern South China Sea: Core MD972151. *Terr. Atmos. Ocean. Sci.*, **10**, 239-254.

Lee, M. Y., K. Y. Wei, and Y. G. Chen, 2001: Astronomically tuned late Pliocene-Pleistocene benthic $\delta^{18}O$ chronostratigraphy for the subtropical western Pacific and its paleoclimatic significance. *West. Pac. Earth Sci.*, **1**, 443-458.

Murray, S. P. and D. Arief, 1988: Throughflow into the Indian Ocean through the Lombok Strait, January 1985 - January 1986. *Nature*, **333**, 444-447.

Pisias, N. G. and D. K. Rea, 1988: Late Pleistocene paleoclimatology of the central equatorial Pacific: Sea surface response to the southeast trade winds. *Paleoceanography*, **3**, 1, 21-37

Széréméta, N., F. Bassinot, Y. Balut, L. Labeyrie, and M. Pagel, 2004: Oversampling of sedimentary series collected by giant corer: Evidence and correction based upon 3.5-kHz chirp profiles. *Paleoceanography*, **19**, PA1005, doi: 10.1029/2002PA000795.

Thierstein, H. R., K. R. Geitzenauer, and B. Molfino, 1977: Global synchroneity of late Quaternary coccolith datum levels: Validation by oxygen isotopes. *Geology*, **5**, 400-404.

Wang, P., 1999: Response of western Pacific marginal seas to glacial cycles: Paleoceanographic and sedimentological features. *Paleoceanography*, **156**, 245-284.

Wang, P., J. Tian, X. Cheng, C. Liu, and J. Xu, 2004: Major Pleistocene stages in a carbon perspective: The South China Sea record and its global comparison. *Paleoceanography*, **19**, PA4005, doi:10.1029/2003PA000991.

Wei, K. Y., T. Z. Chiu, and Y. G. Chen, 2003: Toward establishing a maritime proxy record of the East Asia summer monsoons for the late Quaternary. *Mar. Geol.*, **201**, 67-79.

Wyrtki, K., 1957: The water exchange between the Pacific and Indian Ocean in relation to upwelling processes. *Proc. Pac. Sci. Cong.*, **16**, 61-66.

Wyrtki, K., 1961: Physical oceanography of the Southeast Asian water. NAGA Report, 3, Neyenesch printers, 195 pp.

Wyrtki, K., 1987: Indonesian Through Flow and the associated pressure gradient. *J. Geophys. Res.*, **92**, 12941-12946.

Yan, X. H., C. R. Ho, Q. Zheng, and V. Klemas, 1992: Temperature and size variabilities of the western Pacific warm pool. *Science*, **258**, 1643-1645.